An amperometric uric acid biosensor based on Bis[sulfosuccinimidyl] suberate crosslinker/3-aminopropyltriethoxysilane surface modified ITO glass electrode

Tarushee Ahuja [a,b], Rajesh [b,*], Devendra Kumar [a], Vinod Kumar Tanwar [b], Vikash Sharma [b], Nahar Singh [b], Ashok M. Biradar [b]

[a] Department of Applied Chemistry, Delhi College of Engineering, University of Delhi, Bawana Road, Delhi-110042, India
[b] National Physical Laboratory (Council of Scientific & Industrial Research), Dr. K.S. Krishnan Road, New Delhi-110012, India

Keywords:
Self assembled monolayer
Uricase
Cyclic voltammetry
Impedance

A B S T R A C T

A label free, amperometric uric acid biosensor is described by immobilizing enzyme uricase through a self assembled monolayer (SAM) of 3-aminopropyltriethoxysilane (APTES) using a crosslinker, Bis[sulfosuccinimidyl]suberate (BS^3) on an indium-tin-oxide (ITO) coated glass plate. The biosensor (uricase/BS^3/APTES/ITO) was characterized by, scanning electron microscopy (SEM), atomic force microscopy (AFM) and electrochemical techniques. Chronoamperometric response was measured as a function of uric acid concentration in aqueous solution (pH 7.4). The biosensor shows a linear response over a concentration range of 0.05 to 0.58 mM with a sensitivity of 39.35 μA mM^{-1}. The response time is 50 s reaching to a 95% steady state current value and about 90% of enzyme activity is retained for about 7 weeks. These results indicate an efficient binding of enzyme with the crosslinker over the surface of APTES modified ITO glass plates, which leads to an improved sensitivity and shelf life of the biosensor.

1. Introduction

Uric acid (UA) is the primary end-product of purine metabolism, which is present in biological fluids, such as blood and urine [1]. The normal level of UA in serum is between 0.13 and 0.46 mM (2.18–7.7 mg dL^{-1}) [2], and in urinary excretion is between 1.49 and 4.46 mM (25–74 mg dL^{-11}) [3,4]. The presence of abnormal uric acid levels leads to gout, chronic renal disease, some organic acidemias, leukemia, pneumonia and Lesch–Nyhan syndrome [5]. Hence, the detection of uric acid in body fluids is clinically an important indicator. Different methods like colorimetric, flourometric, spectrophotometric, and electrochemical analyses have been used to determine the concentration of uric acid, but due to simplicity, selectivity, sensitivity and low cost instrumentation, electrochemical methods are favoured.

Uricase is an enzyme that participates in degrading purines by catalyzing the oxidative breakdown of uric acid to allantoin. Uricase catalyzes the in vivo oxidation of uric acid in the presence of oxygen to produce allantoin and CO_2 as oxidation products of uric acid and hydrogen peroxide as a reduction product of O_2. Various types of electrochemical enzyme sensors have been reported to be useful in uric acid determination.

$$\text{Uric acid} + O_2 + H_2O \xrightarrow{\text{uricase}} \text{allantoin} + CO_2 + H_2O_2.$$

The method based on the determination of H_2O_2 has received considerable interest because H_2O_2 can be detected either by its reduction or oxidation. Quantification of UA can be done conveniently by monitoring the concentration of enzymatically generated H_2O_2. Since electrochemical oxidation of H_2O_2 requires high potential, other oxidizable species would interfere in the measurement of UA. Therefore a low potential detection of H_2O_2 is required to avoid the interference from high potential oxidative species. This is done by using a low potential redox probe such as potassium ferricyanide as an electron mediator. Mostly, biological molecule links to an electrode surface by physical adsorption which produces a weak surface modification that cannot resist to stirring and washing and the substrate is not biocompatible and thus inactivates the biomolecule. To prevent this, the substrate surface is modified with self assembled monolayer (SAM) of organic molecules having biocompatibility with biomolecules for efficient coupling [6–9]. In this study, we describe an amperometric biosensor for the quantitative detection of uric acid in aqueous solution. The surface of the indium-tin-oxide (ITO) coated glass plate was modified by forming a SAM of 3-aminopropyltriethoxysilane, which

* Corresponding author. Tel.: +91 11 45609356; fax: +91 11 45609310.
E-mail address: rajesh_csir@yahoo.com (Rajesh).

was subsequently immobilized with uricase through strong amide bonding by utilizing Bis[sulfosuccinimidyl]suberate as a crosslinking reagent. The biosensor (uricase/BS^3/APTES/ITO glass electrode) was characterized by cyclic voltammetry and electrochemical impedance spectroscopy in the presence of $[Fe(CN)6]^{3-}$ as a redox probe.

2. Materials and methods

2.1. Materials

Enzyme uricase (EC 1.7.3.3, 9 units/mg from *Bacillus fastidiosus*) was procured from Sigma Aldrich Corp. 3-aminopropyltriethoxysilane (APTES) was purchased from Merck Chemicals (Germany). Bis[sulfosuccinimidyl]suberate (BS^3) was obtained from Pierce Biotechnology, USA. Uric acid with 99% purity was purchased from CDH, India. Other chemicals were of analytical grade and used without further purification.

2.2. Apparatus

Contact angles were recorded on Drop Shape Analysis System, model DSA10MK2 from Krüss GmbH, Germany. Scanning electron micrographs (SEM) were obtained with a LEO 440 PC, UK based digital scanning electron micrograph at an acceleration voltage of 20.0 kV. Atomic force microscopy (AFM) images were obtained on a VEECO/diCP2, USA scanning probe microscope. Cyclic voltammetry and electrochemical impedance measurements were done on a PGSTAT302N, AUTOLAB instrument from Eco Chemie, The Netherlands. The impedance measurements were performed in the presence of a redox probe $[Fe(CN)_6]^{3-}$ at the scanning frequencies from 0.1 to 100,000 Hz. All measurements were carried out in a conventional three-electrode cell configuration consisting of a working electrode (uricase/BS^3/APTES/ITO), Ag/AgCl reference electrode and platinum foil as a counter electrode.

2.3. Fabrication of uricase/BS^3/APTES/ITO electrode

The ITO coated glass plates ($1 \times 1\,cm^2$) were cleaned by sequential ultrasonic cleaning in soapy water (extran), acetone, ethanol, isopropyl alcohol and distilled water for 10 min each, and dried in vacuum. Then, the cleaned ITO glass plates were put in plasma chamber and exposed to oxygen plasma for 5 min. Finally the ITO glass plates were once again washed with distilled water and dried in vacuum. Cleaned ITO glass plates were immersed in 2% APTES solution prepared in ethanol for 1.5 h, under ambient conditions, to form a SAM. The glass plates were then rinsed with ethanol in order to remove non-bonded APTES from the surface of the substrate and dried under N_2. 5 mM Bis[sulfosuccinimidyl]suberate (BS^3) solution was prepared in sodium acetate buffer, pH 5.0. The APTES coated ITO glass plates were then treated with Bis[sulfosuccinimidyl]suberate (BS^3) solution for 1.0 h, followed by washing with doubled distilled water and dried under N_2. The BS^3 treated APTES/ITO glass plates (BS^3/APTES/ITO) were immersed in uricase solution (~3 U) in phosphate buffer solution (PBS), pH 7.4, for a period of 1.5 h. The excess enzyme was removed by rinsing with PBS and finally dried under N_2, at room temperature and the electrodes (uricase/BS^3/APTES/ITO) were stored at 4 °C.

Table 1
Measurement of contact angle before and after surface modification of substrate and enzyme immobilization.

Type of electrode	Ist drop	IInd drop	IIIrd drop	IVth drop	Vth drop	Mean
Bare ITO	38.14	39.54	39.78	39.97	40.32	39.55
APTES/ITO	73.83	73.47	73.55	73.72	73.29	73.57
Uricase/BS3/ APTES/ITO	89.90	89.67	91.04	90.59	89.85	90.21

3. Results and discussion

Scheme 1 shows the fabrication of uricase/BS^3/APTES/ITO electrode, wherein the free NH_2 groups present at the surface of the APTES/ITO electrode have been utilized for the covalent attachment of uricase using the crosslinking reagent Bis[sulfosuccinimidyl]suberate (BS^3).

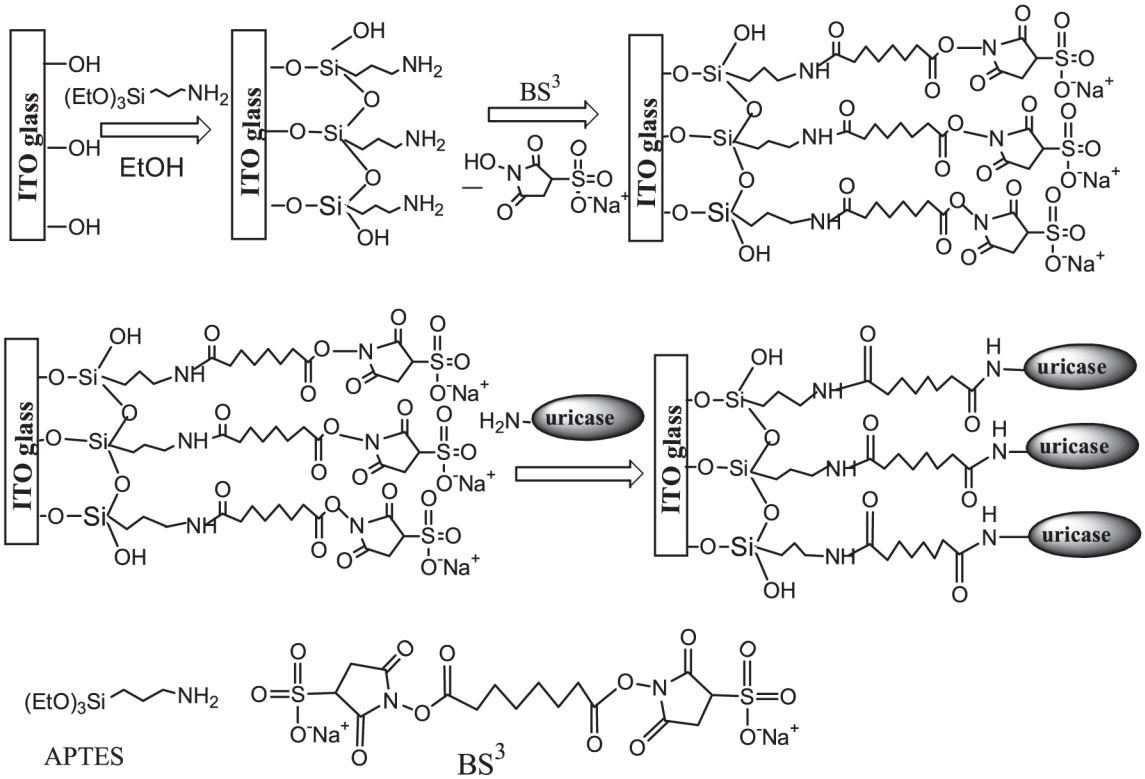

Scheme 1. Scheme illustration of each step of surface modification of ITO glass plate and immobilization of enzyme uricase.

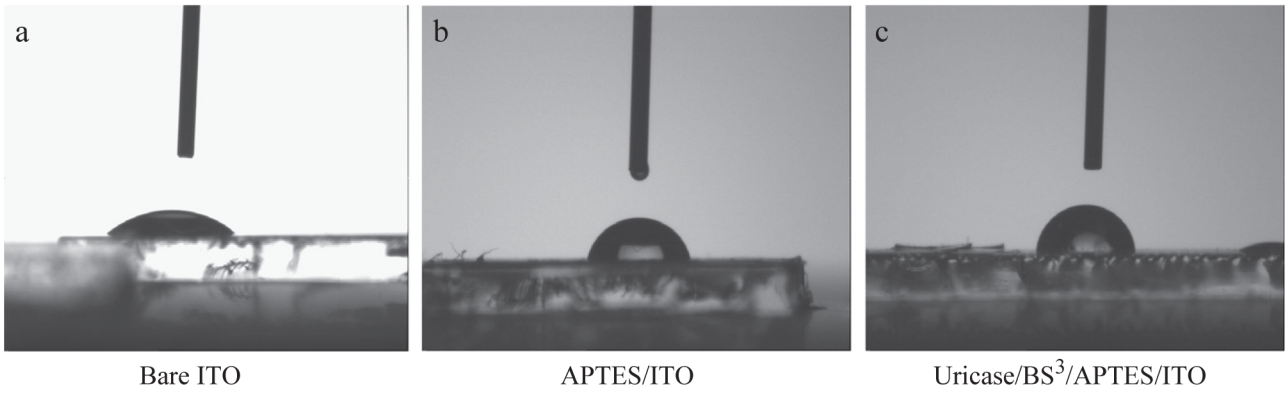

Fig. 1. Contact angle measurement images of (a) ITO coated glass plate; (b) APTES/ITO glass; (c) uricase/BS^3/APTES/ITO glass.

3.1. Contact angle measurement

The various modification steps of the electrode surface were characterized by the static sessile drop method. The drop image was stored and an image analysis system calculated the contact angle (θ) from the shape of the drop. The contact angles for individual modification step of the electrode are listed in Table 1. The hydrophilicity of the surface changes significantly with each step of surface modification. The initial low contact angle value of ~39° (Fig. 1a) was obtained for bare ITO coated glass plate. This hydrophilic character of the surface is due to the presence of surface hydroxyl group. However, after treating the ITO glass plate surface with APTES, the contact angle was found to increase to ~73° (Fig. 1b), a value corresponding to that reported in the previous work [10]. This increase of water drop contact angle with respect to freshly cleaned ITO glass substrate is due to the presence of hydrophobic alkyl chains of APTES molecules. Surface free energy decreases upon silanization with respect to bare substrate (the polar component more than the dispersive component) due to the

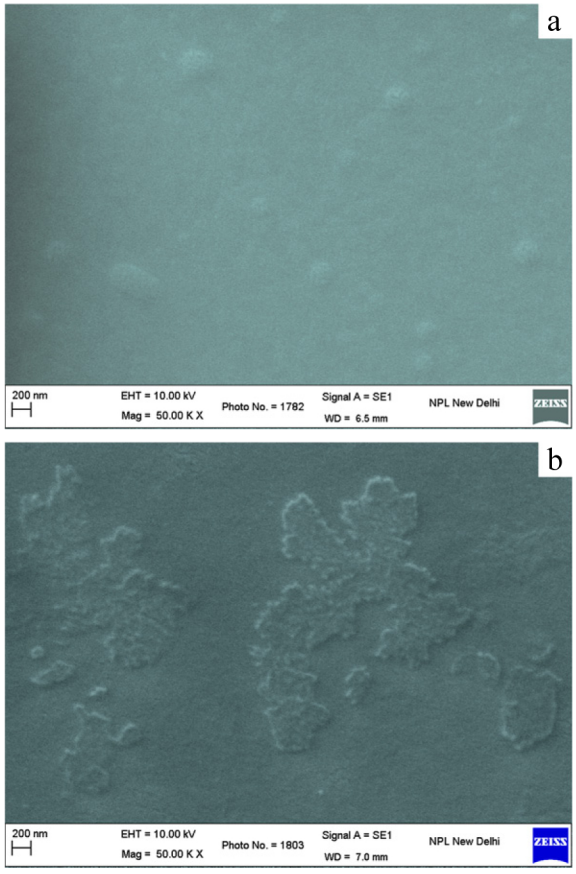

Fig. 2. SEM micrographs of: (a) APTES/ITO glass; (b) uricase/BS^3/APTES/ITO glass at 50,000 magnifications.

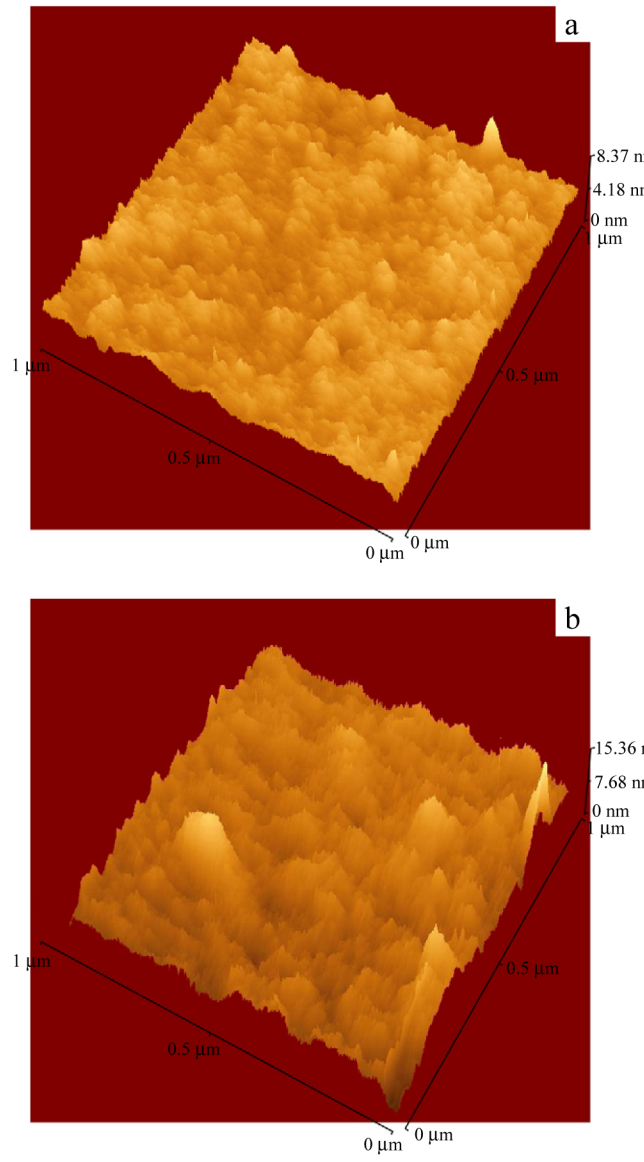

Fig. 3. Contact mode AFM images (1 µm × 11 µm) of: (a) APTES/ITO glass; (b) uricase/BS^3/APTES/ITO glass.

drastic decrease of hydroxyl groups at the surface because of reaction with silane molecules. The glass electrode surface showed even more hydrophobic character after the covalent immobilization of hydrophobic enzyme molecule crosslinked through Bis[sulfosuccinimidyl]suberate with an increased contact angle of 90° (Fig. 1c). These results suggested the formation of a uricase/BS^3/APTES/ITO glass electrode.

3.2. Surface characterization using SEM and AFM

The surface morphology of modified electrode before and after enzyme immobilization was characterized by using scanning electron micrographs and atomic force microscopy (AFM) images. SEM micrograph of the APTES/ITO glass shows a smooth surface (Fig. 2a), whereas in the case of uricase/BS^3/APTES/ITO glass it shows an aggregation of globular shaped crosslinked enzyme molecules (Fig. 2b) over APTES/ITO film. This has further been analyzed by AFM images taken in a contact mode. Fig. 3 shows the AFM images of APTES/ITO films in the presence and absence of uricase. In contrast to the relatively globular shaped surface, the surface morphology of the uricase immobilized APTES/ITO glass exhibits the sharp regular island-like structure. The lateral size of the visible features is strongly affected by the convolution effect between the sample and the AFM tip. An increase of about 8 nm height in the AFM image of uricase modified APTES/ITO glass surface seems to be in accordance with the size of the uricase enzyme molecule [11].

3.3. Electrochemical characterization of uricase/BS^3/APTES/ITO glass electrode

The uricase/BS^3/APTES/ITO glass electrode was characterized by cyclic voltammetry and electrochemical impedance spectroscopy. All electrochemical measurements were performed in PBS solution, pH 7.4, containing 0.1 M KCl and 2 mM $[Fe(CN)_6]^{3-}$. The $[Fe(CN)_6]^{3-}$ probe was used as a marker to investigate the changes in electrode behavior after each surface modification step. Each step of surface modification of ITO glass plate and enzyme immobilization was monitored by cyclic voltammetry. The cyclic voltammogram of the modified electrode before and after the enzyme immobilization is shown in Fig. 4. In all the CV experiments, 3rd cycle was considered as stable one since no significant changes were observed in the subsequent cycles. The bare ITO glass shows a quasi reversible cyclic voltammogram with a peak separation of oxidation and reduction potential (ΔE_p) of 170 mV. On modification with SAM of APTES, it shows a more reversible signal with an increased oxidation and reduction peak current (ΔI_p) of 0.23 mA and a decreased peak separation (ΔE_p) of 128 mV between the cathodic and anodic waves of the redox probe. This reduction in peak 3 potential separation after the formation of APTES layer is attributed to an increased interfacial concentration of the anionic probes ($[Fe(CN)_6]^{3-}$) due to its strong affinity towards the polycatonic (NH_2) layer [12]. However, in contrary to above a decrease in redox peak current (ΔI_p) of 0.19 mA and a significant increase in the peak potential separation (ΔE_p) of 169 mV was observed when APTES modified ITO glass electrode was treated with a crosslinker, Bis[sulfosuccinimidyl]suberate. This increased separation of peak potentials indicates a repulsive interaction of polyanions (SO_3^-) with anionic probe $[Fe(CN)_6]^{3-}$, at the surface interface, conforming the formation of a crosslinker BS^3 layer over the surface of APTES/ITO glass. The CV curve shows a further decrease in redox peak current (ΔI_p) of 0.18 mA and an increased peak separation (ΔE_p) of 214 mV between redox waves after the immobilization of enzyme molecules at the surface of the modified electrode (BS^3/APTES/ITO glass). This may be attributed to the formation of insulating layer of uricase enzyme molecule, at the electrode surface, which perturbs the interfacial electron transfer considerably indicating an efficient covalent bonding of enzyme through a crosslinker BS^3.

Each assembled step involved in the fabrication of uricase/BS^3/APTES/ITO glass electrode was further characterized by electrochemical impedance spectroscopy. The impedance spectroscopy was represented as an equivalent circuit [13] as shown in the inset of Fig. 5. The impedance spectrum, which includes a semicircle portion at higher frequencies, corresponds to the electron-transfer limiting process and a linear part at the low frequencies resulting from diffusion limiting step of the electrochemical process. The ohmic resistance of the electrolyte solution (R_s) and the Warburg impedance (Z_w) represent the bulk properties of the electrolyte solution and diffusion features of the redox probe in solution, respectively. The diameter of the semicircle in the Nyquist plots represents the

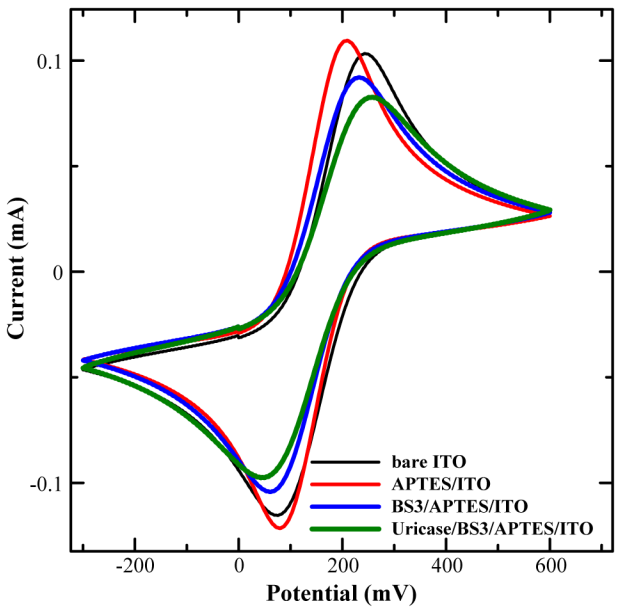

Fig. 4. Cyclic voltammograms of: bare ITO glass; APTES/ITO glass; BS^3/APTES/ITO glass and uricase/BS^3/APTES/ITO glass in 0.1 M KCl solution containing 2 mM $[Fe(CN)_6]^{3-}$; scan rate 25 mV/s; 3rd cycle voltammogram is shown.

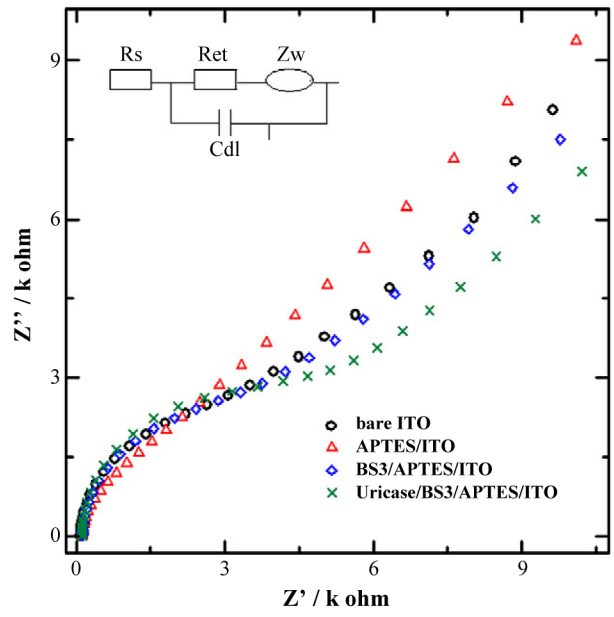

Fig. 5. Nyquist plots obtained for bare ITO glass, APTES/ITO glass, BS^3/APTES/ITO glass and uricase/BS^3/APTES/ITO glass electrodes in 0.1 M KCl solution containing 2 mM $[Fe(CN)_6]^{3-}$. Inset shows a schematic diagram of equivalent circuit for impedance spectroscopy in the presence of redox couple: R_s, resistance of the electrolyte solution; R_{et}, electron-transfer resistance; Z_w, Warburg impedance; C_{dl}, double-layer capacitance.

Table 2
CV peak potential difference (ΔE_p) and the charge-transfer resistance of biosensor before and after each step of ITO glass surface modifications and enzyme immobilization.

Type of electrode	E_{oxi} (mV)	E_{red} (mV)	ΔE_p (mV)	ΔI_p (mA)	Charge-transfer resistance R_{et} (kΩ cm^{-2})
Bare ITO	243	71	170	0.218	3.40
APTES/ITO	207	79	128	0.231	1.41
BS^3/APTES/ITO	232	63	169	0.196	3.20
Uricase/BS^3/APTES/ITO	260	46	214	0.180	5.01

electron-transfer resistance of the layer, and this can be used to describe the interface properties of the modified electrode. Fig. 5 shows the electrochemical impedance spectra of the bare and the modified ITO glass electrode before and after the immobilization of the enzyme uricase and the corresponding electron-transfer resistance values are listed in Table 2. The bare ITO glass shows an electron-transfer resistance (R_{et}) value of 3.40 kΩ. The R_{et} value for APTES/ITO glass was strongly reduced to 1.41 kΩ, which indicates an easy electronic transport at the electrode surface interface after the APTES modification of ITO. However, the treatment of the above electrode surface with a crosslinker, BS^3 and its subsequent immobilization with enzyme uricase results in an increased R_{et} values of 3.20 and 5.01 kΩ, respectively. These results are in conformity with the pattern obtained in cyclic voltammetry measurements, further confirming the formation of the uricase/BS^3/APTES/ITO glass electrode.

3.4. Amperometric response of uricase/BS^3/APTES/ITO glass electrode

Chronoamperometric response studies were conducted with uricase/BS^3/APTES/ITO glass electrode, at a bias voltage of 0.26 V vs Ag/AgCl in PBS; pH 7.4 containing 2 mM $[Fe(CN)_6]^{3-}$. The amperometric response was measured with the successive addition of each 100 μL aliquot of uric acid in 2 mL PBS solution, at an interval of 100 s. The amperometric response obtained is based on an enzymatic reaction mechanism as shown in Scheme 2.

Fig. 6 depicts the chronoamperometric response of uricase/BS^3/APTES/ITO glass electrode along with the reusable response performance as a function of uric acid concentration in aqueous solution. An increasing order of amperometric response was observed after each successive addition of the aliquot of increasing uric acid concentration. The 95% steady state current response to uric acid was obtained in about 50 s.

Fig. 7 shows the steady state current dependence calibration curve to uric acid concentration. The response of the uricase/BS^3/APTES/ITO glass electrode to uric acid was found to be linear in the range of 0.05 to 0.58 mM with a correlation coefficient of 0.993 (n = 5). The lowest detection limit of the electrode was 0.037 mM at a signal-to-noise ratio of 3. The slope of the linearity i.e. the sensitivity of the enzyme electrode towards uric acid was 39.35 μA mM^{-1} cm^{-2}, which is relatively better than the recently reported biosensors and a comparative performance is given in Table 3 [14–27].

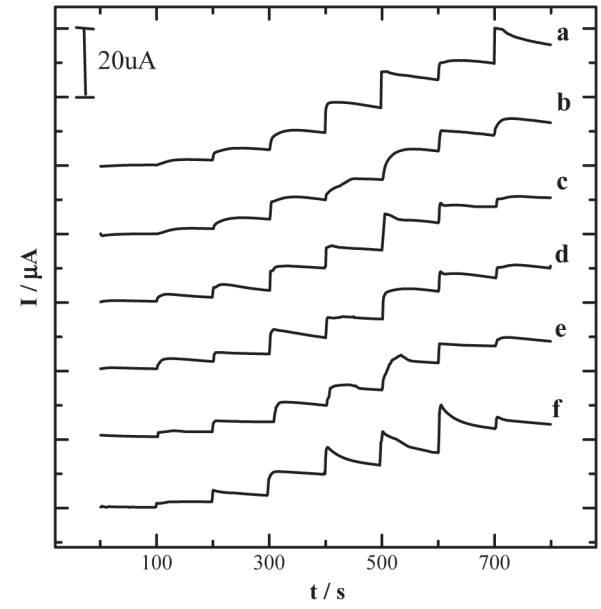

Fig. 6. (a) Chronoamperometric response curve of uricase/BS^3/APTES/ITO with addition of different concentrations of uric acid; repeatability performance of the same electrode from n = 2–6 time (b–f).

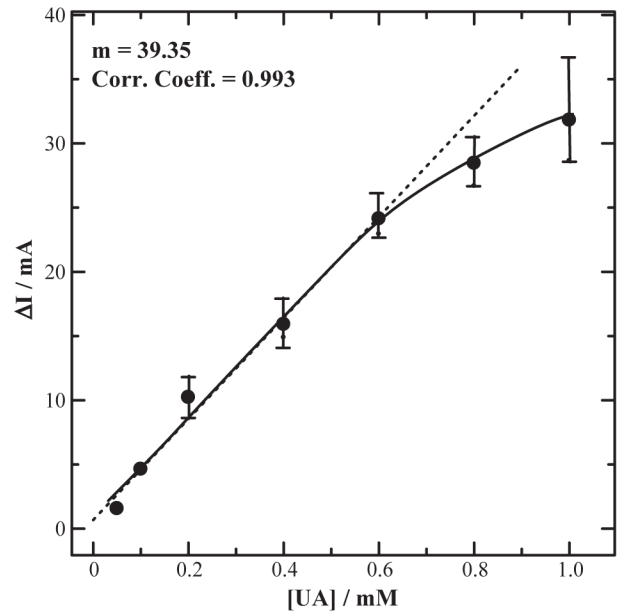

Fig. 7. Steady state current dependence calibration curve of uricase/BS^3/APTES/ITO biosensor to uric acid.

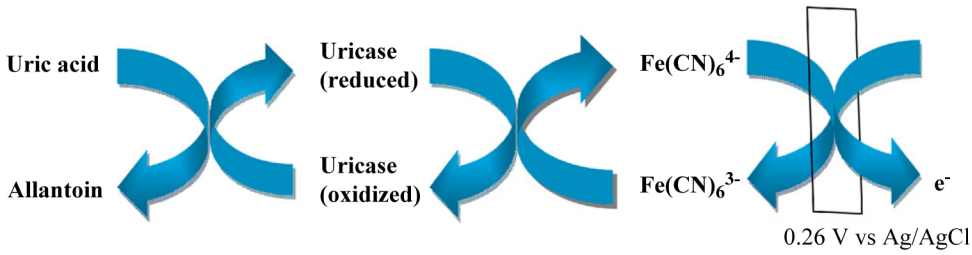

Scheme 2. Enzymatic reaction mechanism of the work of uricase/BS^3/APTES/ITO electrode.

Table 3
Characteristics of some amperometric uric acid sensors.

Matrix	Response time	Stability	Linear range	Sensitivity	Working potential	Reference
SAM of heteroaromatic thiol/Au	–	1 day	1 to 300 μM	0.0149 ± 0.0005 μA mM^{-1}	~0.4 V	[2]
Ir-C	41 s	–	0.1 to 0.8 mM	16.60 μA mM^{-1}	0.25 V	[14]
o-aminophenol-aniline copolymer	–	~50 days	0.0001 to 0.5 mmol dm^{-3}	~2.65 μA mM^{-1}	0.4 V	[15]
Polyaniline	–	~60 days	0.0036 to 1.0 mmol dm^{-3}	~1 μA mM^{-1}	0.4 V	[16]
Polyaniline-polypyrrole	70 s	4 weeks	2.5×10^{-6} to 8.5×10^{-5} M	1.12 μA mM	0.4 V	[17]
CNT/Screen printed carbon electrode	–	2 months	20 to 200 mg/L	0.0568 to 0.0721 μA/mgL^{-1}	0.3 V	[18]
Polyaniline			$1.0\times10-3$ to 1.0 mmol dm^{-3}	<7 μA mM	0.4 V	[19]
poly(allylamine) (PAA)/oly(vinyl sulfate) (PVS)			10^{-6} to 10^{-3}M	<5 μA mM^{-1}	0.6 V	[20]
Zinc sulfide (ZnS) quantum dots		20 days	5.0×10^{-6} to 2.0×10^{-3} mol L^{-1}	2.2 μA mM^{-1}	0.45 V	[21]
Polypropylene			4.82–10.94 mg/dL	0.0029 μA mM^{-1}		[22]
Carbon paste	70 s	>100 days	Up to 100 μmol dm^{-3}		0.34 V	[23]
Self-assembled monolayer of *n*-octanethiolate on Au	20 s		0.15–0.4 mmol dm^{-3}	<1.0 μA mM^{-1}	0 V	[24]
Self-assembled monolayer of 2-(2-mercaptoethylpyr azine) (PET) and 4,4_-dithiodibutyric acid (DTB) on gold (Au) electrode	80–100 s		5–150 μM	3.4 ± 0.08 nA cm^{-2} μM^{-1}	−0.1 V	[25]
Poly(*o*-aminophenol)	37 s	20 days	Up to 1×10^{-4} M		0.05 V	[26]
ZnO nanorods			5.0×10^{-6} to 1.0×10^{-3} mol L^{-1}			[27]
Self assembled monolayer of APTES on ITO	40–50 s	50 days	0.05 to 0.58 mM	39.35 μA mM^{-1}	0.26 V	Present work

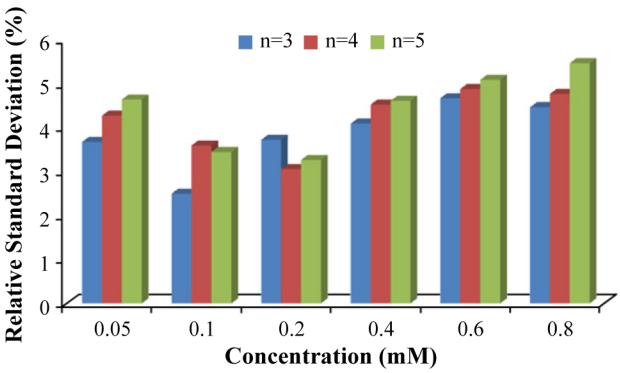

Fig. 8. The reusability performance (n = 3–5) of the uricase/BS^3/APTES/ITO electrode in terms of relative standard deviation at different concentrations of uric acid in PBS.

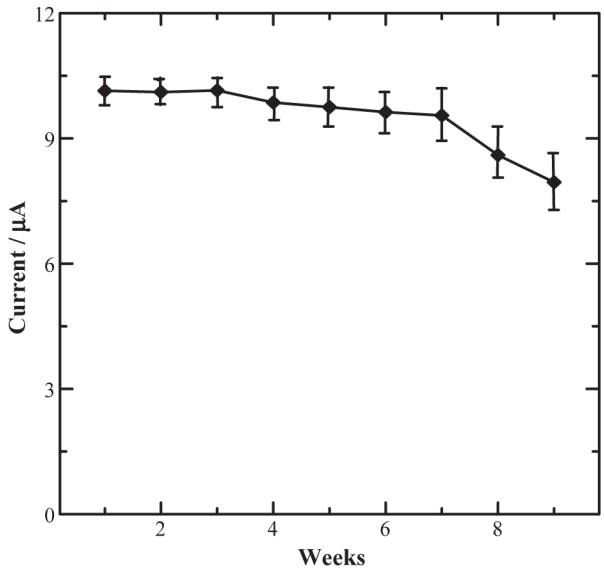

Fig. 9. Effect of storage time on the amperometric response of uricase/BS^3/APTES/ITO electrode.

The reusability of the modified electrode was also tested by conducting the same experiment for several times, under identical conditions. The results were found to be reproducible within a range of the RSD value of 2.5 to 5.1% for 0.05 to 0.6 mM uric acid concentration (n = 3–5), as shown in Fig. 8. The reproducibility of the uricase/BS^3/APTES/ITO glass electrode was investigated in a series of 10 electrodes for 0.2 mM uric acid sample and a relative standard deviation of 7.9% was obtained.

The stability of uricase/BS^3/APTES/ITO glass electrode was studied at an interval of 7 days, when stored at 4–5 °C by continuously monitoring the current response to uric acid, under identical experimental conditions, as shown in Fig. 9. A slow decrement of 5.8% in current response was observed for 50 days of storing after which a sharp decrease of about 15.18% was observed.

5. Conclusion

Uric acid biosensor was fabricated by immobilizing enzyme uricase on SAM of APTES via a crosslinker BS^3 on an ITO glass plate. Uricase/BS^3/APTES/ITO electrode was characterized by electrochemical techniques and amperometric response was studied as a function of uric acid concentration. The biosensor uricase/BS^3/APTES/ITO showed a linear range of 0.05 to 0.58 mM with a lower detection limit of 0.037 mM. The response time was found to be 50 s reaching to a 95% steady state current value. The efficient bonding of enzyme on the electrode surface exhibits an improved sensitivity of 39.35 μA mM^{-1} cm^{-2}. The low cost, easy method of fabrication and high sensitivity makes it advantageous to the recently reported uric acid biosensors.

Acknowledgements

We are grateful to the Director, National Physical Laboratory, Delhi for providing facilities. We are also grateful to the Director, Delhi College of Engineering, Delhi for his kind encouragement and support. One of the authors, T. Ahuja is thankful to the Council of scientific and industrial research, India for financial assistance as SRF.

References

[1] U.S. Eswara, H. Dutt, A. Mottola, Anal. Chem. 46 (1974) 1777.
[2] C.R. Raj, T. Ohsaka, J. Electroanal. Chem. 540 (2003) 69.
[3] R.C. Matos, L. Angnes, M.C.U. Araujo, T.C.B. Saldanha, Analyst 125 (2000) 2011.
[4] R.C. Matos, M.A. Augelli, C.L. Lago, L. Angnes, Anal. Chim. Acta 404 (2000) 151.

[5] C.A. Burtic, E.R. Ashwood, Teitz Textbook of Clinical Chemistry, second ed.WB Saunders, Philadelphia, 1994.
[6] O. Dannenberger, K. Weiss, C. Woll, M. Buck, Phys. Chem. Chem. Phys. 2 (2000) 1509.
[7] D.H. Yun, M.J. Song, S.I. Hong, M.S. Kang, N.K. Min, J. Kor. Phys. Soc. 47 (2005) S445.
[8] R.K. Mendes, R.F. Carvalhal, L.T. Kubota, J. Electroanal. Chem. 612 (2008) 164.
[9] M. Satjapat, R. Sanedrin, F. Zhou, Langmuir 17 (2001) 7637.
[10] S.C. Jain, V.K. Tanwar, V. Dixit, S.P. Verma, S.B. Samanta, Appl. Surf. Sci. 182 (2001) 350.
[11] S. Akgo, N. Ozturka, A.A. Karagozler, D.A. Uyguna, M. Uygun, A. Denizli, J. Mol. Cat. B: Enzy 51 (2008) 36.
[12] J. Zhao, C.R. Bradbury, S. Huclova, I. Potapova, M. Carrara, D.J. Fermin, J. Phys. Chem. B 109 (2009) 22985.
[13] J.B.B. Randles, Disc Faraday Soc. 1 (1947) 11.
[14] Y.C. Luo, J.S. Do, C.C. Liu, Biosens. Bioelectron. 22 (2006) 482.
[15] X. Pan, S. Zhou, C. Chen, J. Kan, Sens Actuators B 113 (2006) 329.
[16] J. Kan, X. Pan, C. Chen, Biosens. Bioelectron. 19 (2004) 1635.
[17] F. Arslan, Sensors 8 (2008) 5492.
[18] H. Xu, G. Li, M. Fu, Y. Wang, J. Liu, Proceeding of the 2005 IEEE 1-4 (2005) 255.
[19] Y. Jiang, A. Wang, J. Kan, Sens. Actuators B 124 (2007) 529.
[20] T. Hoshi, H. Saiki, J. Anzai, Talanta 61 (2003) 363.
[21] F. Zhang, C. Li, X. Li, X. Wang, Q. Wan, Y. Xian, L. Jin, K. Yamamoto, Talanta 68 (2006) 1353.
[22] J.C. Chen, H.H. Chung, C.T. Hsu, D.M. Tsai, A.S. Kumar, J.M. Zen, Sens. Actuators B 110 (2005) 364.
[23] R.F. Dutra, K.A. Moreira, M.I.P. Oliveira, A.N. Araujo, M.C.B.S. Montenegro, J.L.L. Filho, V.L. Silva, Electroanalysis 17 (2005) 701.
[24] T. Nakaminami, S. Ito, S. Kuwabata, H. Yoneyama, Anal. Chem. 71 (1999) 4278.
[25] S. Behera, C.R. Raj, Biosens. Bioelectron. 23 (2007) 556.
[26] E. Miland, A.J. Miranda Ordieres, P. Tunon Blanco, M.R. Smyth, C.O. Fagain, Talanta 43 (1996) 785.
[27] F. Zhang, X. Wang, S. Ai, Z. Sun, Q. Wan, Z. Zhu, Y. Xian, L. Jin, K. Yamamoto, Anal. Chim. Acta 519 (2004) 155.